Adaptive Dynamic Surface Inverse Output Feedback Control for a Class of Hysteretic Systems

Xiuyu Zhang[1], Dan Liu[1], Zhi Li[2], and Chun-Yi Su[2(✉)]

[1] School of Automation Engineering, Northeast Dianli University, Jilin 132012, China
zhangxiuyu80@163.com, 13804428706@139.com
[2] Department of Mechanical and Industrial Engineering, Concordia University, Montreal, QC H3G 1M8, Canada
gavinlizhi@gmail.com, chun-yi.su@concordia.ca

Abstract. In this paper, an robust neural adaptive output-feedback inverse control scheme for a class of hysteretic nonlinear systems is proposed. Firstly, by designing a high-gain observer to estimate the states of the system and cope with the uncertainties of the system, only the output of the control system is required to be measurable. Secondly, the nonlinear function in the systems can totally unknown due to the utilization of the neural networks approximator. Finally, the arbitrarily small $\mathcal{L}_\infty$ norm of the tracking error is achieve by adjusting the initial conditions of the unknown parameters.

Keywords: Inverse control · PI hysteresis model · $\mathcal{L}_\infty$ performance

1 Introduction

Recently, the smart-material based actuators are widely used in the tuning metal cutting system and other ultrahigh-precision positioning devices [1–3]. However, the existence of the hysteresis highly prohibit the control precision [4,5].

The construction of the inverse model of the hysteresis is the commonly method dealing with hysteresis [4–11]. The robust adaptive control method without constructing the hysteresis inverse [5,12–19,30] is the other method. Though there are some existing results [1,12,16–25,28] of modeling and control for the practicable hysteretic nonlinear systems, an output-feedback inverse control scheme is still missing.

In this paper, an adaptive neural output-feedback inverse control is proposed. Firstly, by designing a high-gain observer to estimate the states of the system and cope with the uncertainties of the system, only the output of the control system is required to be measurable. Secondly, the nonlinear function in the systems

This work was supported by the National Natural Science Foundation of China under Grants 61304015.

N. Kubota et al. (Eds.): ICIRA 2016, Part I, LNAI 9834, pp. 646–662, 2016.
DOI: 10.1007/978-3-319-43506-0_56

can totally unknown due to the utilization of the neural networks approximator. Finally, the arbitrarily small $\mathcal{L}_\infty$ norm of the tracking error is achieve by adjusting the initial conditions of the unknown parameters.

The rest of this paper is organized as follows. In Sect. 2, the problem statement, the assumptions and the control objective. Section 3 presents the design procedure. The stability analysis are given in Sect. 4 and the simulation results is shown to illustrate the effectiveness of the proposed method.

2 Problem Statement

We consider a class of nonlinear system preceded by hysteresis as follows:

$$\begin{aligned} \dot{x}_i &= x_{i+1} + f_i(\bar{x}_i) + d_i(t), \\ \dot{x}_n &= b_0 w(u) + f_n(\bar{x}_n) + d_n(t), \\ y &= x_1,\ i = 0, 1, \cdots, n-1, \end{aligned} \tag{1}$$

where $\bar{x}_i := [x_1, x_2, \cdots, x_i]^T \in \mathbb{R}^i$ is the state vector; $f_i(\bar{x}_i)$, $i = 0, 1, \cdots, n$ are the unknown smooth nonlinear functions. τ_i are unknown time delays. $d_i(t)$ are external disturbances. b_0 is an unknown constant parameter. $w \in R$ represents the unknown hysteresis which can be expressed as

$$w(u) = P(u(t)) \tag{2}$$

with u being the input signal of the actuator and Π being the hysteresis operator which will be discussed in details below.

For the system (1), the following assumptions are required:

A1: The disturbances $d_i(t)$, $i = 1, \cdots, n$, satisfy

$$|d_i(t)| \leq \bar{d}_i, \tag{3}$$

where $\bar{d}_i$ are some unknown positive constants.

A2: The desired trajectory y_r is smooth and available with $y_r(0)$ at designer's disposal; $[y_r, \dot{y}_r, \ddot{y}_r]^T$ belongs to a known compact set for all $t \geq 0$.

A3: The sign of b_0 is known, without loss of generality, we assume that $b_0 > 0$ for simplicity.

2.1 The Prandtl-Ishlinskii (PI) Model and Its Inverse

Though a large number of hysteresis models have been reported, in this paper, the PI model which is suitable for describing the hysteresis phenomena in piezoelectric actuators is employed and its corresponding inverse is adopted to mitigate the effects of the hysteresis phenomenon [26].

$$w(t) = P[u](t) \tag{4}$$

with $P[u](t)$ being defined as [26]

$$P[u](t) = p_0 u(t) + \int_0^{\Lambda} p(r) F_r[u](t) dr \tag{5}$$

where r represents the threshold, $p(r)$ is a given density function satisfying $p(r) > 0$ with $\int_0^{\infty} p(r)dr < \infty$, for convenience, $p_0 = \int_0^{D} p(r)dr$ is a constant decided by density function $p(r)$. Λ denotes the upper limit of the integration. Let f_r: $\mathbb{R} \to \mathbb{R}$ be defined by

$$f_r(u, w) = \max(u - r, \min(u + r, w)). \tag{6}$$

Then, the play operator $F_r[u](t)$ satisfies

$$\begin{aligned} &F_r[u](0) = f_r(u(0), 0), \\ &F_r[u](t) = f_r(u(t), F_r[u](t_i)), \\ &\quad \text{for } t_i < t \le t_{i+1} \text{ and } 0 \le i \le N-1, \end{aligned} \tag{7}$$

where $0 = t_0 < t_1 < \cdots < t_N = t_E$ is a partition of $[0, t_E]$ such that the function u is monotone (nondecreasing or non-increasing) on each of the sub-intervals $(t_i, t_{i+1}]$.

To compensate the hysteresis nonlinearities $w(u)$ in (1), the inverse of the PI model is constructed as follows [9]:

$$u(t) = P^{-1} \circ P[u(t)] = P^{-1}[w](t), \tag{8}$$

where $\circ$ denotes the composition operator; $P^{-1}[\cdot]$ is the inverse operator of the PI model with

$$P^{-1}[u](t) = \bar{p}_0 u(t) + \int_0^{\bar{\Lambda}} \bar{p}(r) F_r[u](t) dr, \tag{9}$$

where $\bar{\Lambda}$ is a constant denoting the upper-limit of the integration in (9) and

$$\begin{aligned} \bar{p}_0 &= \frac{1}{p_0}, \\ \bar{p}(r) &= (\varphi^{-1})''(r), \\ \varphi(r) &= \bar{p}_0 r + \int_0^{r} \bar{p}(\xi)(r - \xi) d\xi. \end{aligned} \tag{10}$$

Since in practice, the hysteresis is unknown which implies the density function $p(r)$ needs to be estimated based on the measured data. Here, we use $\hat{p}(r)$ and $\hat{P}[u](t)$, which can be got from experiments data, denotes the estimation of $p(r)$ and $P[u](t)$, respectively. Thus, as that in [26], by applying the composition theorem to the $P[\cdot](t)$ and $\hat{P}^{-1}[\cdot](t)$ as in [9], yields

$$P \circ \hat{P}^{-1}[u_d](t) = \phi'(0)u_d(t) + \int_0^{\Lambda} \phi''(r)F_r[u_d](t)dr, \tag{11}$$

with u_d being the control signal to be designed. $\phi(r) = p \circ \hat{p}^{-1}(r)$, $p(r)$ and $\hat{p}^{-1}(r)$ being the initial loading curves of the $P[\cdot](t)$ and $\hat{P}^{-1}[\cdot](t)$.

Considering (11) and the equality $F_r[u_d](t) + E_r[u_d](t) = u_d(t)$ given in [26], it follows that

$$w(t) = \phi'(\Lambda)u_d + d_b(t), \tag{12}$$

where $\phi^{'}(\Lambda)$ is a positive constant, $E_r(\cdot)$ is the stop operator of PI model. Due to $|E_r(\cdot)| < \Lambda$ (see [9]), the term $d_b(t) = -\int_0^{\Lambda} \phi''(r)E_r[u_d](t)dr$ is bounded and satisfies

$$|d_b(t)| \leq D \tag{13}$$

with D being a positive constant. Therefore, from (11) and (12), the analytical error $e(t)$ expression can be obtained as follows

$$\begin{aligned} e(t) &= w(t) - u_d(t) \\ &= [\phi'(\Lambda) - 1]u_d + d_b(t). \end{aligned} \tag{14}$$

Now, substituting (12) into (1), we have

$$\begin{aligned} \dot{x}_i &= x_{i+1} + f_i(\bar{x}_i) + d_i(t),\ i = 0, 1, \cdots, n-1 \\ \dot{x}_n &= b_\Lambda u_d + f_n(\bar{x}_n) + b_0 d_b(t) + d_n(t), \\ y &= x_1, \end{aligned} \tag{15}$$

where b_Λ is a positive constant satisfying

$$b_\Lambda = b_0\phi'(\Lambda). \tag{16}$$

2.2 Radial Basis Function Neural Networks

In this paper, the radial basis function neural network (RBFNNs) with a linear in the weights property will be employed to approximate a continuous function on the compact sets under the following Lemma 1.

Lemma 1 [27]: RBFNNs are universal approximators in the sense that given any real continuous function $f : \Omega_\xi \to \mathbb{R}$ being a compact set with $\Omega_\xi \subset \mathbb{R}^q$, ξ being the NNs input and q denoting the input dimension. For any $\varepsilon_m > 0$, by appropriately choosing σ and $\zeta_k \in \mathbb{R}^q$, $k = 1, \ldots, N$, then, there exists an RBFNN such that

$$\begin{aligned} f(\xi) &= \psi^T(\xi)\vartheta^* + \varepsilon, \\ &\forall \xi \in \Omega_\xi \subset \mathbb{R}^n, |\varepsilon| \leq \varepsilon_m, \end{aligned} \tag{17}$$

where ϑ^* is an optimal weight vector of $\vartheta = [\vartheta_1, \ldots, \vartheta_N] \in \mathbb{R}^N$ and defined as

$$\vartheta^* = \arg\min_{\vartheta \in \mathbb{R}^n} \left\{ \sup_{\xi \in \Omega_\xi} |Y(\xi) - f(\xi)| \right\}, \tag{18}$$

$\psi(\xi) = [\psi_1(\xi), \ldots, \psi_N(\xi)] \in \mathbb{R}^N$ is an basis function vector. Generally, the so-called Gaussian function is used as basis function in the following form:

$$\begin{aligned} \psi_k(\xi) = & \exp\left(-\frac{||\xi - \zeta_k||}{2\sigma^2}\right), \\ \text{with } \sigma & > 0, k = 1, \ldots, N, \end{aligned} \tag{19}$$

where $\zeta_k \in \mathbb{R}^n$ is a constant vector called the center of the basis function, and σ is a real number called the width of the basis function and ε being approximation error, satisfying

$$\varepsilon = f(\xi) - \vartheta^{*\mathrm{T}} \psi(\xi). \tag{20}$$

Then, by using Lemma 1 and (17), the RBFNNs are used as the approximators to approximate the unknown continuous functions in (17) as follows:

$$\begin{aligned} f_i(\bar{x}_i) &= \psi_i^T(\xi_i)\vartheta_i^* + \varepsilon_i, \\ &\text{for } i = 1, \cdots, N \end{aligned} \tag{21}$$

with ε_i being any positive constants denoting the neural networks approximated errors and

$$\xi_i := (\hat{\hat{x}}_1, \cdots, \hat{\hat{x}}_i,), \ i = 1, \cdots, n, \tag{22}$$

where $\hat{\hat{x}}_1, \cdots, \hat{\hat{x}}_i$ are the estimations of the state variables $x_1, \cdots, x_i$, and will be introduced in the following section.

Now, substituting (21) into (15), we have

$$\begin{aligned} \dot{x}_i &= x_{i+1} + \psi_i^T(\xi_i)\vartheta_i^* + \delta_{i0} \\ &\quad + \varepsilon_i + d_i(t), \\ \dot{x}_n &= b_\Lambda u_d + \psi_n^T(\xi_n)\vartheta_n^* + \delta_{n0} + \varepsilon_n \\ &\quad b_0 d_b(t) + d_n(t), \\ y &= x_1, \ i = 0, 1, \cdots, n-1 \end{aligned} \tag{23}$$

from which system (1) eventually can be expressed as the following state-space form

$$\begin{aligned} \dot{x} &= Ax + \Psi^T(\xi)\vartheta^* + bu_d + D_b \\ &\quad + \delta_0 + \varepsilon + d, \\ y &= e_1^T x, \end{aligned} \tag{24}$$

where

$$A = \begin{bmatrix} 0 & 1 & & 0 \\ 0 & & \ddots & \\ \vdots & & & 1 \\ 0 & \cdots & 0 & 0 \end{bmatrix}, b = \begin{bmatrix} 0 \\ \vdots \\ 0 \\ b_\Lambda \end{bmatrix},$$

$$d = \begin{bmatrix} d_1(t) \\ \vdots \\ d_{n-1}(t) \\ d_n(t) \end{bmatrix}, \varepsilon = \begin{bmatrix} \varepsilon_1 \\ \vdots \\ \varepsilon_{n-1} \\ \varepsilon_n \end{bmatrix},$$

$$\delta_0 = \begin{bmatrix} \delta_{10} \\ \vdots \\ \delta_{n-10} \\ \delta_{n0} \end{bmatrix}, D_b = \begin{bmatrix} 0 \\ \vdots \\ 0 \\ d_b(t) \end{bmatrix},$$

$$\vartheta^* = \begin{bmatrix} \vartheta_1^* \\ \vdots \\ \vartheta_{n-1}^* \\ \vartheta_n^* \end{bmatrix} \subset \mathbb{R}^{\Sigma_{i=1}^n N_n},$$

$$\Psi^T(\xi) = \begin{bmatrix} \psi_1 & & \\ & \ddots & \\ & & \psi_n \end{bmatrix} \tag{25}$$

with $\psi_1 = [\psi_{1,1}(\xi_1), \cdots, \psi_{1,N_1}(\xi_1)]$, $\psi_n = [\psi_{n,1}(\xi_n), \cdots, \psi_{n,N_n}(\xi_n)]$, and N_i, $i = 1, \cdots, n$ being defined in (19).

The control objective is to develop an adaptive neural output-feedback dynamic surface inverse control scheme for a class of nonlinear hysterestic system such that the output y well tracks the reference signal y_r with the $\mathcal{L}_\infty$ norm of the tracking error and all the signals of the closed loop system are uniformly bounded.

3 Observer Based Adaptive DSIC Design

3.1 High-Gain K-Filter Observer

Now, (24) can be transformed as the following

$$\begin{aligned} \dot{x} &= A_0 x + qy + \Psi^T(\xi)\vartheta^* + bu_d + B, \\ y &= e_1^T x, \end{aligned} \tag{26}$$

by letting

$$B = D_b + \delta_0 + \varepsilon + d, \tag{27}$$

and

$$A_0 = A - qe_1^T = \begin{bmatrix} -q_1 & 1 & & \\ -q_2 & & \ddots & \\ \vdots & & & 1 \\ -q_n & 0 & \cdots & 0 \end{bmatrix}$$
$$\text{with } q = \begin{bmatrix} q_1 \\ q_2 \\ \vdots \\ q_n \end{bmatrix}, \tag{28}$$

where A_0 is a Hurwitz matrix by properly choosing the vector q.

Inspired by the previous work [13,14], the following high-gain K-Filter is construct to estimate the states x in systems (26).

$$\dot{v}_0 = kA_0v_0 + \Phi^{-1}e_nu_d, \tag{29}$$
$$\dot{\xi}_0 = kA_0\xi_0 + kqy, \tag{30}$$
$$\dot{\Xi} = kA_0\Xi + \Phi^{-1}\Psi^T, \tag{31}$$

where $k \geq 1$ is a positive design parameter, e_n denotes the n-th coordinate vector in $\mathbb{R}^n$, and

$$\Phi = diag\{1, k, \cdots, k^{n-1}\}. \tag{32}$$

From (29)–(32), the estimated states vector is as the following:

$$\hat{x} = \Phi\xi_0 + \Phi b_\Lambda v_0 + \Phi\Xi\vartheta^*. \tag{33}$$

To proceed, we define the estimation error

$$\epsilon = x - \hat{x}. \tag{34}$$

It is easy to verify that

$$A = k\Phi A\Phi^{-1},$$
$$k\Phi qe_1^T\Phi^{-1} = k\Phi qe_1^T \tag{35}$$

with $e_1^T = [1, 0, \cdots, 0]^T$. Then, we have

$$\dot{\epsilon} = A\epsilon - k\Phi q\epsilon_1 + B, \tag{36}$$

where ϵ_1 is the first entry of ϵ and B is defined in (27).

Lemma 2: Let the high-gain K-filters be defined by (29)–(31) and the quadratic function

$$V_\epsilon := \epsilon^T P\epsilon, \tag{37}$$

where $P = (\Psi^{-1})^T \bar{P} \Psi^{-1}$ with $\bar{P} = \bar{P}^T$ is positive define matrix ($\bar{P} > 0$) satisfying

$$A_0^T \bar{P} + \bar{P} A_0 = -2I, \tag{38}$$

where A_0 is defined by (28). Let

$$\begin{aligned} \zeta_\epsilon &:= \frac{k}{\lambda_{\max}(\bar{P})}, \\ \delta_\epsilon &:= k \left(\frac{\|\bar{P}\| \, \|B\|_{\max}}{k^n} \right)^2, \end{aligned} \tag{39}$$

where $\|B\|_{\max}$ is the maximum value of $\|B\|$. Then, for any $k \geq 1$, we have

$$\dot{V}_\epsilon \leq -\zeta_\epsilon V_\epsilon + \delta_\epsilon. \tag{40}$$

Proof: See [13] for more details.

It should be noted that because b_Λ and ϑ^* in (33) are unknown, $\hat{x}(t)$ is unavailable. Therefore, the actual state estimation is

$$\hat{\hat{x}} = \Phi \xi_0 + \Phi \hat{b}_\Lambda v_0 + \Phi \Xi \hat{\vartheta}, \tag{41}$$

where $\hat{b}_\Lambda$ and $\hat{\vartheta}$ are the estimations of b_Λ and ϑ^*, and will be given in details in the next section.

3.2 Dynamic Surface Inverse Controller Design

By using the states observer in (29)–(31), a robust adaptive dynamic surface inverse control scheme will be given with the following structure of the controller (Fig. 1).

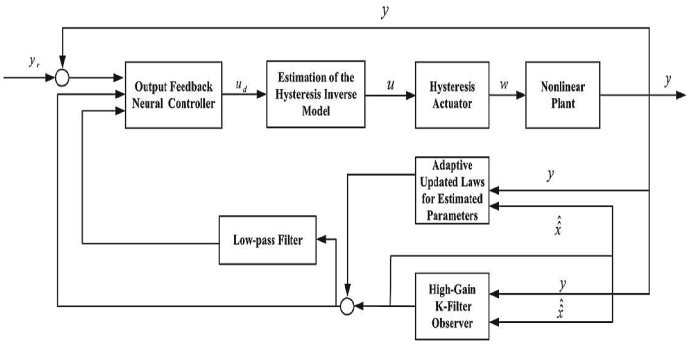

Fig. 1. The structure of the proposed control scheme

Based on the above controller structure, the procedures of the controller design are as follows:

Step 1: Define the first surface error as

$$S_1 = y - y_r, \tag{42}$$

whose time derivative by considering (24) is

$$\begin{aligned}\dot{S}_1 &= \dot{y} - \dot{y}_r \\ &= x_2 + \psi_1^T(\xi_1)\vartheta_1^* + \delta_{10} \\ &\quad +\varepsilon_1 + d_1 - \dot{y}_r.\end{aligned} \tag{43}$$

From (34), we have

$$\begin{aligned}x_2 &= \hat{x}_2 + \epsilon_2 \\ &= k\xi_{0,2} + b_\Lambda k v_{0,2} + k\Xi_{(2)}\vartheta^* + \epsilon_2,\end{aligned} \tag{44}$$

where $\Xi_{(2)}$ denotes the second row of Ξ. Then, it follows that

$$\begin{aligned}\dot{S}_1 &= k\xi_{0,2} + b_\Lambda k v_{0,2} + k\Xi_{(2)}\vartheta^* \\ &\quad +\vartheta_1^{*T}\psi_1(\xi_1) - \dot{y}_r + \epsilon_2 + \delta_{10} \\ &\quad +\varepsilon_1 + d_1\end{aligned} \tag{45}$$

with ξ_1 being defined in (22). Note that $\vartheta_1^{*T}\psi_1(\xi_1) = \vartheta^{*T}\Psi_{(1)}^T$ with $\Psi_{(1)}^T$ denoting the first row of Ψ^T, then, (45) can be rewritten as

$$\begin{aligned}\dot{S}_1 &= k\xi_{0,2} + b_\Lambda k(v_{0,2} - \bar{v}_{0,2}) + b_\Lambda k\bar{v}_{0,2} \\ &\quad +\vartheta^{*T}(k\Xi_{(2)} + \Psi_{(1)})^T - \dot{y}_r + \epsilon_2 \\ &\quad +\delta_{10} + \varepsilon_1 + d_1,\end{aligned} \tag{46}$$

where $\bar{v}_{0,2}$ is the first virtual control signal to be designed. Let $\bar{v}_{0,2}$ be of the following form

$$\bar{v}_{0,2} = \hat{\zeta}\bar{v}_{0,2}^{'} \tag{47}$$

with $\hat{\zeta}$ being the estimation of $\zeta = 1/b_\Lambda$ and

$$\begin{aligned}\bar{v}_{0,2}^{'} &= [-l_1 S_1 - k\xi_{0,2} - \hat{\vartheta}^T(k\Xi_{(2)} \\ &\quad +\Psi_{(1)})^T + \dot{y}_r]/k,\end{aligned} \tag{48}$$

where $\hat{\vartheta}$, is the estimate of ϑ^*. The updated laws of $\hat{\zeta}$ and $\hat{\vartheta}$ are as follows

$$\dot{\hat{\zeta}} = -\gamma_\zeta(k\bar{v}_{0,2}^{'}S_1 + \sigma_\zeta\hat{\zeta}) \tag{49}$$

$$\dot{\hat{\vartheta}} = \gamma_\vartheta[(k\Xi_{(2)} + \Psi_{(1)})^T S_1 - \sigma_\vartheta\hat{\vartheta}] \tag{50}$$

Let $\bar{v}_{0,2}$ pass through the a first-order filter to obtain a new state variable z_2

$$\tau_2 \dot{z}_2 + z_2 = \bar{v}_{0,2},\ z_2(0) = \bar{v}_{0,2}(0), \tag{51}$$

where τ_2 is the time constant of the first-order filter.

Step 2: Define the second surface error

$$S_2 = v_{0,2} - z_2, \tag{52}$$

whose time derivative by considering $\dot{v}_{0,2}$ in (29) is

$$\begin{aligned} \dot{S}_2 &= -kq_2 v_{0,1} + kv_{0,3} - \dot{z}_2 \\ &= -kq_2 v_{0,1} + k(v_{0,3} - \bar{v}_{0,3}) \\ &\quad + k\bar{v}_{0,3} - \dot{z}_2. \end{aligned} \tag{53}$$

Then the virtual control $\bar{v}_{n-\rho,i+1}$ is chosen as

$$\bar{v}_{0,3} = (-l_2 S_2 + kq_2 v_{0,1} + \dot{z}_2 - \hat{b}_\Lambda k S_1)/k, \tag{54}$$

where l_2 is a positive design parameters and $\hat{b}_\Lambda$ is the estimation of b_Λ defined in (16). The updated law of $\hat{b}_\Lambda$ is designed as

$$\dot{\hat{b}}_\Lambda = \gamma_b (k S_1 S_2 - \sigma_b \hat{b}_\Lambda) \tag{55}$$

Let $\bar{v}_{0,3}$ pass through the a first-order filter to obtain a new state variable z_3:

$$\tau_3 \dot{z}_3 + z_3 = \bar{v}_{0,3},\ z_3(0) = \bar{v}_{0,3}(0). \tag{56}$$

where τ_3 is the time constant of the first-order filter.

Step *i* $(3 \le i \le n-1)$: Define the i-th surface error

$$S_i = v_{0,i} - z_i, \tag{57}$$

whose time derivative by considering $\dot{v}_{0,i}$ in (29) is

$$\begin{aligned} \dot{S}_i &= -kq_i v_{0,1} + kv_{0,i+1} - \dot{z}_i \\ &= -kq_i v_{0,1} + k(v_{0,i+1} - \bar{v}_{0,i+1}) \\ &\quad + k\bar{v}_{0,i+1} - \dot{z}_i. \end{aligned} \tag{58}$$

Then the virtual control $\bar{v}_{0,i+1}$ is chosen as

$$\bar{v}_{0,i+1} = (kq_i v_{0,1} + \dot{z}_i - l_i S_i)/k, \tag{59}$$

where l_i, $i = 3, \cdots, n-1$, are positive design parameters. Let $\bar{v}_{0,i+1}$ pass through the a first-order filter to obtain a new state variable z_{i+1}:

$$\begin{aligned} \tau_{i+1} \dot{z}_{i+1} + z_{i+1} &= \bar{v}_{0,i+1}, \\ z_{i+1}(0) &= \bar{v}_{0,i+1}(0). \end{aligned} \tag{60}$$

where τ_{i+1} is the time constant of the first-order filter.

Step n: Define the n-th surface error

$$S_n = v_{0,n} - z_n, \tag{61}$$

whose derivative by considering $\dot{v}_{0,n}$ in (29) is

$$\dot{S}_n = -kq_n v_{0,1} + k^{1-n} u_d - \dot{z}_n. \tag{62}$$

The actual control u_d appears in this step and is chosen as

$$u_d = k^{n-1}(kq_n v_{0,1} + \dot{z}_n - l_n S_n), \tag{63}$$

where l_n is a positive design parameter.

4 Stability and $\mathcal{L}_\infty$ Tracking Performance Analysis

In this section, the stability and performance analysis for the proposed adaptive output feedback DSIC scheme will be discussed. Now, we are ready to present the main theorem of this paper to analyize the stability and achieve the $\mathcal{L}_\infty$ performance of the tracking error.

Theorem 1: Consider the closed loop system including the time-delay system (1) with hysteresis nonlinearity described by (4), the updated laws of the unknown parameters (36), (37), (55), and the control law (63) with respect to Assumptions A1–A3. Then, for any given positive number p, if $V(0)$ in (68) satisfies $V(0) \leq p$,

(a) all the signals of the closed loop system are uniformly bounded and can be made arbitrarily small by properly choosing the design parameters $k, l_1, \cdots, l_n$, the time constant $\tau_2, \cdots, \tau_n$, and the update law parameters γ_ϑ, σ_ϑ, γ_ζ, σ_ζ, γ_b, σ_b.

(b) the $\mathcal{L}_\infty$ performance the of the tracking error S_1 can be obtained and arbitrary small and satisfy

$$\|S_1\|_\infty \leq \sqrt{\frac{C_2}{C_1} + \frac{2}{k^2}\lambda_{\max}(\bar{P})\,\|\epsilon(0)\|^2} \tag{64}$$

where C_1 is a design parameter and C_2 is a positive constant that will be given in the proof of Theorem 1.

Proof: First of all, define

$$y_i = z_i - \bar{v}_{n-\rho,i},\ \ i = 2, \cdots, \rho. \tag{65}$$

Then, we have

$$\left|\dot{y}_2 + \frac{y_2}{\tau_2}\right| \leq B_2(S_1, \ldots, S_n, y_2, \cdots, y_n, \tilde{b}_\Lambda, \tilde{\zeta}, \tilde{\vartheta}, y_r, \dot{y}_r, \ddot{y}_r, \epsilon), \tag{66}$$

where B_2 is a continuous function. Similarly, it can be verified that for $i = 2, \cdots, n-1$,

$$\left|\dot{y}_{i+1} + \frac{y_{i+1}}{\tau_{i+1}}\right| \leq B_{i+1}(S_1, \ldots, S_\rho, y_2, \cdots, y_n, \tilde{b}_\Lambda, \tilde{\zeta}, \tilde{\vartheta}, y_r, \dot{y}_r, \ddot{y}_r, \epsilon), \tag{67}$$

where B_{i+1} are some continuous functions. For the analysis of stability, define the Lyapunov function as:

$$V = \frac{1}{2}\sum_{i=1}^{n} S_i^2 + \frac{1}{2}\sum_{i=1}^{n-1} y_{i+1}^2 + \frac{1}{2\gamma_\vartheta}\tilde{\vartheta}^T\tilde{\vartheta} + \frac{b_\Lambda}{2\gamma_\zeta}\tilde{\zeta}^2 + \frac{1}{2\gamma_b}\tilde{b}_\Lambda^2 + V_\epsilon \tag{68}$$

where $\tilde{b}_\Lambda = \hat{b}_\Lambda - b_\Lambda$, $\tilde{\vartheta}$ and $\tilde{\zeta}$ have been introduced as in [13], V_ϵ is a quadratic function concerning the high-gain K-Filter observer error ϵ which has been given in Lemma 2.
Define the following compact sets

$$\Omega_1 = \left\{(y_r, \dot{y}_r, \ddot{y}_r) : y_r^2 + \dot{y}_r^2 + \ddot{y}_r^2 \leq G_0\right\},$$
$$\Omega_2 = \left\{\begin{array}{c} \sum_{i=1}^{n} S_i^2 + \sum_{i=1}^{n-1} y_{i+1}^2 + \frac{1}{\gamma_\vartheta}\tilde{\vartheta}^2 \\ \frac{1}{\gamma_b}\tilde{b}_\Lambda + \frac{b_\Lambda}{\gamma_\zeta}\tilde{\zeta}^2 + 2\epsilon^T P\epsilon \leq 2p \end{array}\right., \tag{69}$$

where G_0 and p are positive constant. Note that $\Omega_1 \times \Omega_2$ is also compact. Therefore, as that in [29], the continuous functions B_{i+1}, in (66) and (67) have maximum values on $\Omega_1 \times \Omega_2$, say, $M_{i+1}, i = 1, \cdots, n-1$. Then, from (??)–(67), it follows that

$$y_{i+1}\dot{y}_{i+1} \leq -\frac{y_{i+1}^2}{\tau_{i+1}} + \frac{y_{i+1}^2 M_{i+1}^2}{2\varsigma} + \frac{\varsigma}{2}, \quad i = 1, \ldots, \rho-1, \tag{70}$$

where ς is any positive constant.
From (68), the time derivative of the Lyapunov function V is

$$\dot{V} = \sum_{i=1}^{n} S_i\dot{S}_i + \sum_{i=1}^{n-1} y_{i+1}\dot{y}_{i+1} + \frac{1}{\gamma_\vartheta}\tilde{\vartheta}^T\dot{\tilde{\vartheta}} + \frac{b_\Lambda}{\gamma_\zeta}\tilde{\zeta}\dot{\tilde{\zeta}} + \frac{1}{\gamma_b}\tilde{b}_\Lambda\dot{\tilde{b}}_\Lambda + \dot{V}_\epsilon \tag{71}$$

Then, by choosing the design parameters as

$$\begin{gathered} k \geq \lambda_{\max}(\bar{P})C_1 + \frac{\lambda_{\max}(\bar{P})}{2\lambda_{\min}(\bar{P})}, \\ l_1 \geq (\frac{b_\Lambda k}{2} + \frac{k^2}{2} + C_1), \\ l_2 \geq k + C_1, l_n \geq \frac{k}{2} + C_1, \\ l_i \geq \frac{3k}{2} + C_1,\ i = 3, \cdots, n-1, \\ \frac{1}{\tau_2} \geq \frac{b_\Lambda k}{2} + \frac{M_2^2}{2\varsigma} + C_1, \\ \frac{1}{\tau_{i+1}} \geq \frac{k}{2} + \frac{M_{i+1}^2}{2\varsigma} + C_1, \\ i = 2, \cdots, n-1, \\ \sigma_\vartheta \gamma_\vartheta \geq 2C_1, \sigma_b \gamma_b \geq 2C_1, \\ \sigma_\zeta \gamma_\zeta \geq 2C_1, \end{gathered} \tag{72}$$

where C_1 is a positive constant. Then, it follows that

$$\dot{V} \leq -2C_1 V + C_2 \tag{73}$$

with

$$\begin{aligned} C_2 = \frac{(n-1)\varsigma}{2} + \frac{\sigma_\vartheta}{2}\vartheta^{*T}\vartheta^* \\ + \frac{b_\Lambda \sigma_\zeta}{2}\zeta^2 + \frac{\sigma_b}{2}b_\Lambda^2 \\ + \frac{1}{2}(\delta_{10}^2 + \varepsilon_1^2 + d_1^2) + \delta_\epsilon, \end{aligned} \tag{74}$$

and C_1 satisfying

$$C_1 \geq \frac{C}{2p}. \tag{75}$$

Then, $\dot{V} \leq 0$ when $V = p$, which implies that $V(t) \leq p$ is an invariant set or in other words, if $V(0) \leq p$, then $V(t) \leq p$, for all $t \geq 0$. Therefore, Thus, all the signals of the closed loop system are uniformly bounded.

Furthermore, let $y_r(0) = y(0)$. Then, $S_1(0) = 0$. Now, we set the initial condition of the K-Filter as

$$\begin{aligned} v_0(0) &= 0, \\ \xi_{0,1}(0) &= y(0), \\ \Xi(0) &= 0, \end{aligned} \tag{76}$$

and $\hat{\vartheta}(0) = 0$, $\hat{\zeta}(0) = 0$, $\hat{b}_\Lambda(0) = 0$ in the updated laws. Then, it follows that

$$V(t) \leq \frac{C_2}{2C_1} + \frac{1}{k^2}\lambda_{\max}(\bar{P}) \left\|\epsilon(0)\right\|^2. \tag{77}$$

Therefore, the $\mathcal{L}_\infty$ norm of the tracking error satisfies

$$\begin{aligned}\|S_1\|_\infty &= \sup_{t\geq 0}|S_1| = \|x_1 - y_r\|_\infty \\ &\leq \sqrt{\frac{C_2}{C_1} + \frac{2}{k^2}\lambda_{\max}(\bar{P})\left\|\epsilon(0)\right\|^2}.\end{aligned} \tag{78}$$

(78) implies the $\mathcal{L}_\infty$ norm of the tracking error $\|S_1\|_\infty$ can be arbitrarily small by choosing sufficient large design parameters in (72). This completes the proof. ■

5 Simulation Results

We consider the following general second-order system:

$$\begin{aligned}\dot{x}_1 &= x_2 + 0.8x_1^2 + 0.2x_1x_1(t-0.4) + 0.1\cos(t),\\ \dot{x}_2 &= w + 2x_1x_2 + 0.5x_1(t-0.5)x_2(t-1),\\ y &= x_1,\end{aligned} \tag{79}$$

where w is the ASPI hysteresis described by (4) with density functions being selected as $p(r) = 0.4e^{-0.015r^2}$, $r \in [0, 10]$; the initial value of state-variables are chosen as $x_1(0) = x_2(0) = 0$. The high-gain K-filters are as follows

$$\begin{aligned}\dot{v}_0 &= kA_0v_0 + \Phi^{-1}e_nu_d,\ v(0) = 0,\\ \dot{\xi}_0 &= kA_0\xi_0 + kqy,\ \xi_0(0) = 0,\\ \dot{\Xi} &= kA_0\Xi + \Phi^{-1}\Psi^T,\ \Xi(0) = 0,\end{aligned} \tag{80}$$

where

$$\begin{aligned}k = 2, q &= \begin{bmatrix}q_1\\ q_2\end{bmatrix} = \begin{bmatrix}3\\ 2\end{bmatrix},\\ A_0 &= \begin{bmatrix}-q_1 & 1\\ -q_2 & 0\end{bmatrix}, \Phi^{-1} = \begin{bmatrix}1 & 0\\ 0 & 1/k\end{bmatrix}.\end{aligned} \tag{81}$$

where $\psi(\xi) = [\psi^1(\xi), \psi^2(\xi), \ldots, \psi^N(\xi)]^{\mathrm{T}} \in R^N$ is RBFNNs function vector. For NNs $\psi_1(\xi_1)$, we choose 5 nodes with the centers of the basis functions ζ_j, $j = 1, \cdots, 5$, being evenly spaced in $[-1, +1]$, and the width $\eta_j = 1$, $j = 1, \cdots, 5$; and $\xi_1 = \hat{\hat{x}}_1$. For NNs $\psi_2(\xi_2)$, we choose 11 nodes with the centers of the basis functions ζ_j, $j = 1, \cdots, 11$, being evenly spaced in $[-2, +2]$, and the width $\eta_j = 1$, $j = 1, \cdots, 11$; and $\xi_1 = (\hat{\hat{x}}_1, \hat{\hat{x}}_2)$. Then, $\Psi^T(\xi) = diag\{\psi_1, \psi_2\}$.

In this simulation, the design parameter are chosen as $l_1 = 30$, $l_2 = 40$, $k = 1.5$, $\gamma_\zeta = 3$, $\sigma_\zeta = 0.004$, $\gamma_\vartheta = 10$, $\sigma_\vartheta = 0.05$, $\gamma_b = 9$, $\sigma_b = 0.0002$. The initial value of the system states are selected as $x_1(0) = x_2(0) = 0$. The initial value of the updated parameters are chosen as $\hat{\zeta}(0) = \hat{\vartheta}(0) = \hat{b}_\Lambda(0) = 0$. The control objective of this simulation is to make the output of the control system follows the desired trajectory $y_r = \sin t$.

According to the above design procedures and the selections of the parameters, the simulation results are shown in Figs. 2, 3 4 and 5. From Fig. 2, the output of the control system $y = x_1$ well tracks the desired trajectory $y_r = \sin t$ when the ASPI hysteresis inverse compensator described in (8)–(10) is applied. Figure 3 shows the trajectories of the tracking errors under two circumstances: with (solid

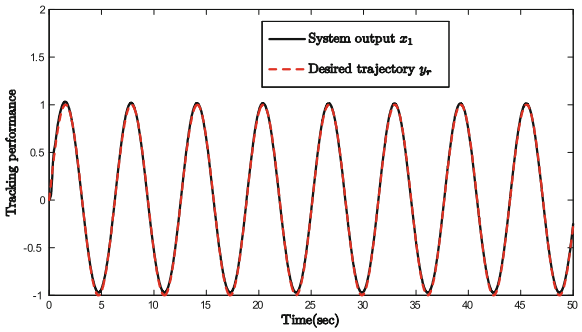

Fig. 2. Tracking performance

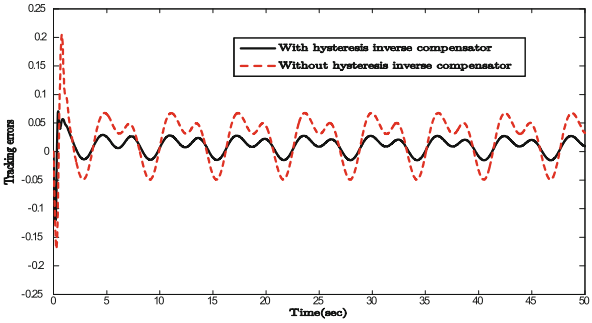

Fig. 3. Tracking errors

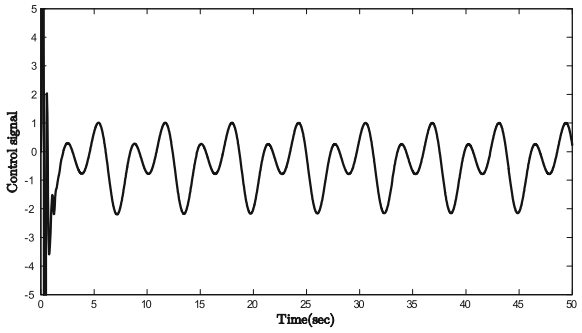

Fig. 4. Control signal

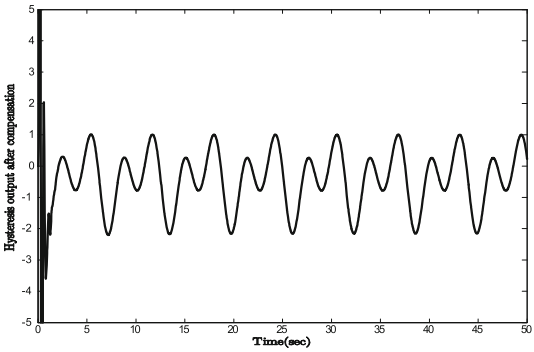

Fig. 5. Hysteresis output after compensation

line) and without (dashed line) considering the ASPI hysteresis inverse compensator. Figure 4 illustrates the trajectory of control signal u_d. Figure 5 illustrates the hysteresis output w after ASPI inverse compensation.

References

1. Gu, G.Y., Zhu, L.M., Su, C.-Y.: Modeling and compensation of asymmetric hysteresis nonlinearity for piezoceramic actuators with a modified Prandtl-Ishlinskii model. IEEE Trans. Ind. Electron. **61**(3), 1583–1595 (2014)
2. Xu, Q., Li, Y.: Micro-/nanopositioning using model predictive output integral discrete sliding mode control. IEEE Trans. Ind. Electron. **59**(2), 1161–1170 (2012)
3. Xu, Q.: Robust impedance control of a compliant microgripper for high-speed position/force regulation. IEEE Trans. Ind. Electron. **62**(2), 1201–1209 (2015)
4. Tao, G., Kokotovic, P.V.: Adaptive control of plants with unknown hysteresis. IEEE Trans. Autom. Control **40**(12), 200–212 (1995)
5. Su, C.Y., Wang, Q.Q., Chen, X.K., Rakheja, S.: Adaptive variable structure control of a class of nonlinear systems with unknown Prandtl-Ishlinskii hysteresis. IEEE Trans. Autom. Control **50**(12), 2069–2074 (2005)
6. Liu, S., Su, C.-Y., Li, Z.: Robust adaptive inverse control of a class of nonlinear systems with Prandtl-Ishlinskii hysteresis model. IEEE Trans. Autom. Control **59**(8), 2170–2175 (2014)
7. Xie, W., Fu, J., Yao, H., Su, C.-Y.: Neural network-based adaptive control of piezoelectric actuators with unknown hysteresis. Int. J. Adapt. Control Signal Process. **23**, 30–54 (2009)
8. Chen, X., Hisayama, T., Su, C.-Y.: Adaptive control for uncertain continuous-time systems using implicit inversion of Prandtl-Ishlinskii hysteresis representation. IEEE Trans. Autom. Control **55**(10), 2357–2363 (2010)
9. Krejci, P., Kuhnen, K.: Inverse control of systems with hysteresis and creep. Proc. Inst. Elect. Eng. **148**(3), 185–192 (2001)
10. Li, Z., Su, C.-Y., Chen, X.: Modeling and inverse adaptive control of asymmetric hysteresis systmes with applications to magnetostrictive actuator. Control Eng. Pract. **33**(12), 148–160 (2014)

11. Zhou, J., Wen, C., Li, T.: Adaptive output feedback control of uncertain nonlinear systems with hysteresis nonlinearity. IEEE Trans. Autom. Control **57**(10), 2627–2633 (2012)
12. Gu, G.Y., Zhu, L.M., Su, C.Y., Ding, H.: Motion control of piezoelectric positioning stages: modeling, controller design, and experimental evaluation. IEEE/ASME Trans. Mechatron. **18**(5), 1459–1471 (2013)
13. Zhang, X., Lin, Y., Wang, J.: High-gain observer based decentralised output feedback control for interconnected nonlinear systems with unknown hysteresis input. Int. J. Control **86**(6), 1046–1059 (2013)
14. Zhang, X., Lin, Y.: An adaptive output feedback dynamic surface control for a class of nonlinear systems with unknown backlash-like hysteresis. Asian J. Control **15**(2), 489–500 (2013)
15. Zhang, X., Su, C.-Y., Lin, Y., Ma, L., Wang, J.: Adaptive neural network dynamic surface control for a class of time-delay nonlinear systems with hysteresis inputs and dynamic uncertainties. IEEE Trans. Neural Netw. Learn. Syst. **26**, 2844–2860 (2015). doi:10.1109/TNNLS.2015.2397935
16. Huang, S., Tan, K.K., Lee, T.H.: Adaptive sliding-mode control of piezoelectric actuators. IEEE Trans. Ind. Electron. **56**(9), 3514–3522 (2009)
17. Shieh, H.-J., Hsu, C.-H.: An adaptive approximator-based backstepping control approach for piezoactuator-driven stages. IEEE Trans. Ind. Electron. **55**(5), 1729–1738 (2008)
18. Xu, Q.: Identification and compensation of piezoelectric hysteresis without modeling hysteresis inverse. IEEE Trans. Ind. Electron. **60**(9), 3927–3937 (2013)
19. Chen, X., Hisayama, T.: Adaptive sliding-mode position control for piezo-actuated stage. IEEE Trans. Ind. Electron. **55**(11), 3927–3934 (2008)
20. Wong, P.K., Xu, Q., Vong, C.M., Wong, H.C.: Rate-dependent hysteresis modeling and control of a piezostage using online support vector machine and relevance vector machine. IEEE Trans. Ind. Electron. **59**(4), 1988–2001 (2012)
21. Tang, H., Li, Y.: Development and active disturbance rejection control of a compliant micro-/nanopositioning piezostage with dual mode. IEEE Trans. Ind. Electron. **61**(3), 1475–1492 (2014)
22. Abidi, K., Sabanovic, A.: Sliding-mode control for high-precision motion of a piezostage. IEEE Trans. Ind. Electron. **54**(1), 629–637 (2007)
23. Huang, D., Xu, J.-X., Venkataramanan, V., Huynh, T.C.T.: High-performance tracking of piezoelectric positioning stage using current-cycle iterative learning control with gain scheduling. IEEE Trans. Ind. Electron. **61**(2), 1085–1098 (2014)
24. Goldfarb, M., Celanovic, N.: Modeling piezoelectric stack actuators for control of micromanipulation. IEEE Control Syst. **17**(3), 69–79 (1997)
25. Adriaens, H.J.M.T.S., De Koning, W.L., Banning, R.: Modeling piezoelectric actuators. IEEE/ASME Trans. Mechatron. **5**(4), 331–341 (2000)
26. Brokate, M., Sprekels, J.: Hysteresis and Phase Transitions. Springer, New York (1996)
27. Sanner, R.M., Slotine, J.-J.E.: Gaussian networks for direct adaptive control. IEEE Trans. Neural Netw. **3**(6), 837–863 (1992)
28. Tong, S.C., Li, Y.: Adaptive fuzzy output feedback tracking backstepping control of strict-feedback nonlinear systems with unknown dead zones. IEEE Trans. Fuzzy Syst. **20**(1), 168–180 (2012)
29. Swaroop, D., Hedrick, J.K., Yip, P.P., Gerdes, J.C.: Dynamic surface control for a class of nonlinear systems. IEEE Trans. Autom. Control **45**(10), 1893–1899 (2000)
30. Zhong, J., Yao, B.: Adaptive robust precision motion control of apiezoelectric positioning stage. IEEE Trans. Control Syst. Technol. **16**(5), 1039–1046 (2008)